Silicon Monomer Formation and Surface Patterning of Si(001)−2 × 1 Following Tetraethoxysilane Dissociative Adsorption at Room Temperature

ARTICLE *in* THE JOURNAL OF PHYSICAL CHEMISTRY C · DECEMBER 2013

Impact Factor: 4.77 · DOI: 10.1021/jp407411k

THE JOURNAL OF PHYSICAL CHEMISTRY C

Article

pubs.acs.org/JPCC

Silicon Monomer Formation and Surface Patterning of Si(001)-2 × 1 Following Tetraethoxysilane Dissociative Adsorption at Room Temperature

Héloise Tissot,[†,‡,§] Jean-Jacques Gallet,*[,†,‡,§] Fabrice Bournel,[†,‡,§] Ahmed Naitabdi,[†,‡,§] Debora Pierucci,[†,‡,§] Federica Bondino,[∥] Elena Magnano,[∥] François Rochet,[†,‡,§] and Fabio Finocchi[⊥,○]

[†]Laboratoire de Chimie Physique Matière et Rayonnement, Sorbonne Universités, UPMC Univ Paris 06, UMR 7614, 11 rue Pierre et Marie Curie, 75231 Paris Cedex 05, France

[‡]CNRS, UMR 7614, LCPMR, 75005 Paris, France

[§]Synchrotron SOLEIL, L'Orme des Merisiers, Saint-Aubin, Gif-sur-Yvette, France

[∥]IOM-CNR, TASC Laboratory, s.s. 14 km 163.5, Basovizza, 34149 Trieste, Italy

[⊥]Institut des Nano-Sciences de Paris, Sorbonne Universités, UPMC Univ Paris 06, UMR 7588, 4 place Jussieu, 75252 Paris Cedex 05, France

[○]CNRS, UMR 7588, INSP, 75005 Paris, France

S *Supporting Information*

ABSTRACT: The adsorption of tetraethoxysilane (TEOS, $Si[OC_2H_5]_4$) on the Si(001)-2 × 1 surface at 300 K is studied through a joint experimental and theoretical approach, combining scanning tunneling microscopy (STM) and synchrotron radiation X-ray photoelectron spectroscopy (XPS) with first-principles simulations within the density functional theory (DFT). XPS shows that all Si−O bonds within the TEOS molecules are broken upon adsorption, releasing one Si atom per dissociated molecule, while the ethoxy ($-OC_2H_5$) groups form new Si−O bonds with surface Si dimers. A comparison between experimental STM images and DFT adsorption configurations shows that the four ethoxy groups bind to two second-neighbor silicon dimers within the same row, while the released silicon atom is captured as a monomer on an adjacent silicon dimer row. Additionally, the surface displays alternate ethoxy- and Si adatom-covered rows as TEOS coverage increases. This patterning, which spontaneously forms upon TEOS adsorption, can be used as a template for the nanofabrication of one-dimensional self-organized structures on Si(001)-2 × 1.

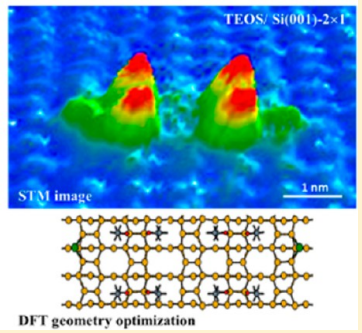

INTRODUCTION

Since the beginning of the silicon surface chemistry studies in the mid-1980s,[1] the grafting of organic monomolecular arrays on silicon surfaces via the direct formation of Si−C bonds (both in ultrahigh vacuum and wet conditions[2,3]) has stimulated a considerable interest, essentially because of promising applications in molecular electronics.[4,5] Organosilanes (by definition a silane that contains at least one Si−C bond) are also widely used to form self-assembled monolayers on silicon substrates.[6−8] Within this class of molecules, alkoxysilanes ($R_nSi(OR)_{4-n}$) are not attached directly to clean silicon surfaces, but rather to native silicon oxide ones, either through the direct reaction of surface Si−OH with the hydrolyzable (alkoxy) terminations of the molecules or via a more complex process involving the participation of molecular water. Recently, Fan and Lopinski[9] investigated the reaction of an alkoxysilane, in the absence of molecular water, with the surface hydroxyls of the water-reacted surface (H,OH)-Si(001)-2 × 1.[10]

However, the grafting of alkoxysilanes directly on clean Si(001)-2 × 1 is an emerging field of study. Recently, we examined the reaction of *n*-propyl-triethoxy-silane (PTES, $Si[OCH_2CH_3]_3[CH_2CH_2CH_3]$) on Si(001)-2 × 1 at room temperature and under ultrahigh vacuum conditions.[11] Using X-ray Photoemission Spectroscopy (XPS), we observed that PTES adsorbs dissociatively at room temperature via the scission of Si−O bonds. However, the actual number of broken Si−O bonds in PTES after dissociative adsorption remained elusive due to the presence of nonidentical ligands (one propyl and three ethoxy groups).[11]

The latter issue prompted us to examine how a simpler molecule with four identical ligands, tetraethoxysilane (TEOS, $Si[OCH_2CH_3]_4$), reacts with Si(001)-2 × 1. Many unknowns remain about the microscopic processes governing the adsorption of TEOS on Si(001)-2 × 1 at room temperature and under UHV conditions (see, e.g., the review by Rauscher[12]). In fact most studies focus on the deposition and electrical/structural characterization of SiO_2 films using TEOS

Received: July 25, 2013
Revised: December 20, 2013
Published: December 30, 2013

   dx.doi.org/10.1021/jp407411k | *J. Phys. Chem. C* 2014, 118, 1887−1893

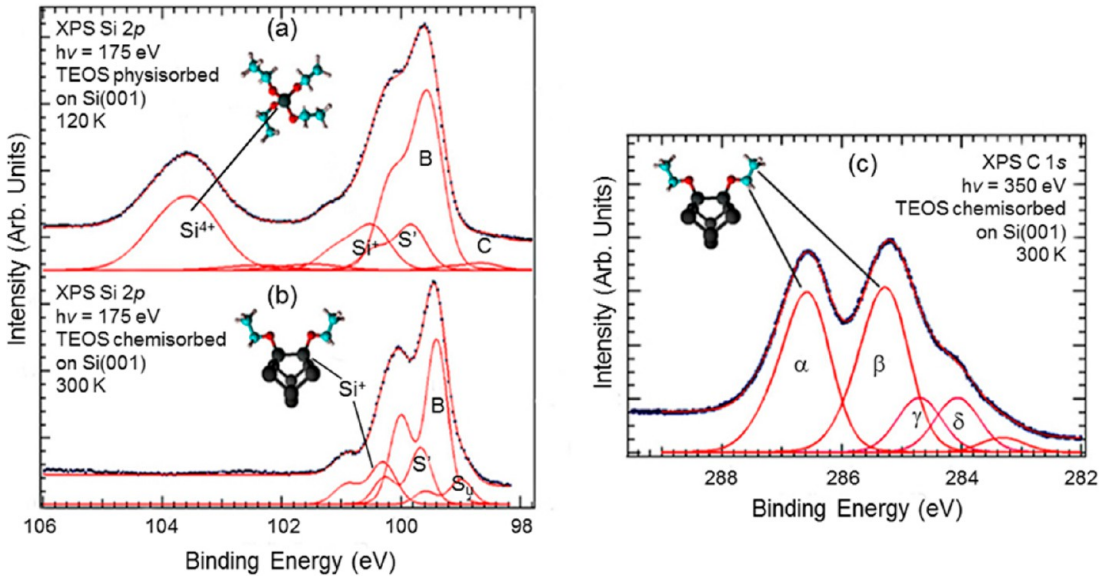

Figure 1. (a) Si 2p XPS spectrum ($h\nu$ = 175 eV) of TEOS physisorbed on Si(001)-2 × 1 surface (n^+-doped, 0.003 Ω × cm) (clean surface exposed to 6.75 L of TEOS, 15 min, 10^{-8} mbar, at 120 K). (b) Si 2p XPS spectrum of TEOS chemisorbed on Si(001)-2 × 1 surface (surface exposed to 4.5 L of TEOS, 10 min, 10^{-8} mbar, at 300 K). (c) C 1s XPS spectrum ($h\nu$ = 350 eV) of TEOS chemisorbed on Si(001)-2 × 1 surface, at room temperature. The BE is referenced with respect to the Fermi level.

as a precursor.[13−15] The few published works devoted to the reaction of TEOS with the clean silicon surface date back to almost two decades ago. As an example, Bonzel et al.[16] in a Mg K_α XPS and ultraviolet photoelectron spectroscopy (UPS) study concluded that no adsorbed TEOS could be detected on the Si(001) surface after its exposure to 10^{-7}−10^{-3} mbar of TEOS at 300 K. According to these authors, adsorption occurs when the molecule is thermally activated. An earlier work, based on high resolution electron energy loss spectroscopy (HREELS), studied also the deposition of TEOS onto Si(001)-2 × 1, but different deposition conditions were used.[17] The adsorption of TEOS, made at 90 K, was followed by annealings at room temperature and above. There is a clear indication that TEOS is chemisorbed on the surface, but in our opinion, the vibrational spectra do not provide clear-cut information on the nature of the bond breaking (Si−O or C−O) since the Si−C stretching mode is indiscernible from the Si−O one.

In order to unravel the microscopic mechanisms governing the interaction of TEOS with clean Si(001), we combine the information about the chemical bond delivered by synchrotron radiation XPS with that about the adsorption sites produced by atomically resolved scanning tunneling microscopy (STM). Electronic structure calculations based on density functional theory (DFT) and STM image simulations gave a sound support to understand the experimental STM images. Finally we discuss how the dissociation mode of TEOS, rather unusual for a silane species,[12] leads to a spontaneous patterning of the Si(001)-2 × 1 surface.

EXPERIMENTAL AND THEORETICAL METHODS

Sample Preparation. Highly doped (phosphorus) n^+-type Si(001) wafers (resistivity 0.003 Ω·cm, $N_D \approx 2 \times 10^{19}$ cm^{-3}) were cleaned from their native oxide by flash annealing (Joule effect) at 1100 °C after prolonged degassing at 600 °C in ultrahigh vacuum. The silicon surface was then exposed to tetraethoxysilane (TEOS, commercial product Sigma-Aldrich, purum 98%) by dosing in situ. Doses are expressed in Langmuirs (1 L = 10^{-6} Torr × s, where 0.75 Torr = 1 mbar).

Core-Level Photoemission Spectroscopy Using Synchrotron Radiation. Core-level photoemission measurements were performed at BACH Beamline, ELETTRA synchrotron facility (Trieste). Linearly polarized light in the 35−1600 eV range is provided by a high energy APPLE II helical undulator. The photon dispersion system is based on a Padmore variable angle spherical grating monochromator. Photoemission spectra are measured by means of a modified 150 mm VSW hemispherical electron analyzer with a 16-channels detector. In the adopted geometry, the photon beam direction is perpendicular to the sample surface (the polarization was contained in the surface plane) and the photoelectron emission angle was at 60° from the sample surface.

The O 1s, C 1s, and Si 2p core-level spectra were recorded at photon energies of 640, 350, and 175 eV, respectively. The overall experimental resolution is better than 100 meV for O 1s and C 1s and better than 80 meV for Si 2p. The zero binding energy (BE) (i.e., the Fermi level) was taken at the leading edge of a clean molybdenum foil in electrical contact with the silicon crystal.

STM Experiments. We used the variable temperature scanning tunneling microscope STM XA (Omicron Nano-Technology) of the UPMC campus (Paris). The occupied-states STM images are obtained in constant current mode (I = 100 pA), at a sample voltage (V_{bias}) of −2 V at room temperature. The chemically etched tungsten tip is cleaned by heating in UHV prior to STM measurements.

Computational Details. The electronic structure and the adsorption energies of different adsorption configurations of TEOS on the silicon surface were computed within the density functional theory (DFT), adopting the generalized gradient approximation to the exchange and correlation energy.[18] The interaction between the ionic cores and the valence electrons was described through ultrasoft pseudopotentials, as implemented in the VASP code.[19,20] A Si slab consisting of 8 atomic layers, with lateral dimensions corresponding to a (8 × 4) two-

dx.doi.org/10.1021/jp407411k | J. Phys. Chem. C 2014, 118, 1887−1893

dimensional (2D) unit cell, was adopted in the simulations (see Supporting Information section B for more computational details).

RESULTS AND DISCUSSION

We start with the determination of the nature of the chemical bonding of TEOS on Si(001), as provided by XPS. In this experiment, the clean reconstructed surface is exposed to TEOS at 120 and 300 K for doses of 6.75 and 4.5 L, respectively. All core-level spectra necessary to discuss the adsorption modes are presented in Figure 1a,b (Si 2p after TEOS adsorption at 120 and 300 K) and Figure 1c (C 1s after adsorption at 300 K). Details on the curve fitting procedure are given in the Supporting Information (section A). The core-level spectra are plotted against a BE scale referenced to the Fermi level. The Si $2p_{3/2}$ BE of the bulk silicon component varies with coverage and substrate temperature. At room temperature, the Si $2p_{3/2}$ BE of the bulk component is found at 99.35 eV. It shifts to 99.40 eV after TEOS adsorption at 300 K (due to a reduction of the upward band bending) and at 99.55 eV for TEOS physisorbed at 120 K, the increase in BE being largely due to a surface photovoltage effect[21] that flattens the bands at cryogenic temperature. The O 1s peak (300 K), not shown here, is given in Figure S1 of the Supporting Information (section A).

Leaving out the case of deposition at 120 K, for which solid molecular TEOS is formed (TEOS desorbs above 195 K[12,17]), the first observation is the presence of carbon and oxygen after exposure to 4.5 L of TEOS at room temperature, together with the appearance of an oxidation state (see below for more details) in the surface sensitive[22] Si 2p spectrum ($h\nu$ = 175 eV, kinetic energy ≈ 75 eV). This is in stark contrast with the negative result of Bonzel et al.[16] The lack of surface sensitivity of conventional XPS in the measurement of the Si 2p spectrum ($h\nu$ = 1253.6 eV, kinetic energy ≈ 1.1 keV) likely explains the difference.

The determination of the oxidation state of the central atom of the molecule, denoted Si^T, by XPS is crucial to conclude about the nature and the precise number of broken chemical bonds in the TEOS molecule. If we consider that dissociative chemisorption on the surface occurs via cleavage of Si−O bonds as for PTES,[11] the number of remaining oxygen neighbors around Si^T depends on the number of cleaved bonds, according to the scheme:

$$Si^T(OC_2H_5)_4 + n(\equiv Si^S) \rightarrow Si^T(OC_2H_5)_{4-n} + n(\equiv Si^S{-}OC_2H_5)$$

where $\equiv Si^S$ is a tricoordinated silicon of the surface and n an integer less than or equal to 4. The number of oxygen ligands $i = 4 - n$ around the central atom Si^T determines its oxidation state, denoted Si^{i+}. However, the number of oxygen ligands around Si^T is not affected if the O−C bond is broken, i.e., the oxidation state of Si^T remains Si^{4+}. The key spectroscopic feature of the Si 2p spectra is the BE position of the oxidation states. In the case of the Si/SiO_2 interface, each oxidation state is associated with a well-defined Si $2p_{3/2}$ surface core-level shifts (SCLS), referenced to the BE of the bulk Si $2p_{3/2}$ component. With i being the oxidation state (the number of O ligands), the SCLS scales as ∼0.9 × i eV, the chemical shifts being additive.[23−26]

However, in the case of the TEOS molecule, the ethoxy ($-OC_2H_5$) ligand may induce a chemical shift different from that due to oxygen in siloxane bridges (Si−O−Si) in SiO_2. For instance, the BE shift per ethoxy ligand in gas phase ethoxysilane $Si[CH_3]_n[OC_2H_5]_{4-n}$ is reported to be only ∼+0.4 eV,[27] which suggests that the nature of second neighbor atoms (C versus Si) may impact the BE shifts. Therefore, it is crucial to measure the BE shift of the intact TEOS molecule (Si^{4+} oxidation state) with respect to the substrate component. Thus, we produced physisorbed TEOS molecules by exposing the surface to the gas at 120 K (6.75 L). The Si 2p XPS spectrum is shown in Figure 1a (the fitting parameters are collected in Table S1 of the Supporting Information). We observe a component with SCLS of +3.88 eV that we ascribe to the intact physisorbed molecule. The SCLS of the intact molecule (a Si^{4+} state) is nearly equal to that of the Si^{4+} state at the Si/SiO_2 interface (∼+3.6 eV[23,24]). Since the second neighbor effect (Si versus C) is not present, as suggested by the gas phase data, we can clearly state that the SCLS of partially decomposed products via Si−O bond breaking should also follow the additivity rule (∼0.9 eV/oxygen ligand). Therefore, we introduce two components in the fitting procedure, with fixed SCLS of ∼+1.8 eV (Si^{2+}) and ∼+2.7 eV (Si^{3+}). Their overall intensity is almost negligible, below 4% of the total spectral weight and is within the detectability limit. On the other hand, we clearly see a Si^{1+} state with a SCLS of ∼+0.92 eV. After heating the sample back to room temperature, the Si^{1+} component is the only oxidation state remaining visible. The Si 2p spectrum is then similar to that obtained after TEOS exposure at room temperature (Figure 1b). The annealing experiment confirms that no chemisorbed Si^{4+} species is produced at 120 K and that the Si^{1+} component results from the dissociation of some TEOS molecules on the surface at 120 K, the product being similar to that formed directly at room temperature (see below).

The Si 2p XPS spectrum (Figure 1b) of the surface exposed to TEOS at room temperature is characterized by the absence of the Si^{4+} component at ∼+3.9 eV. As discussed before, physisorbed molecules cannot remain on the surface at this temperature. Neither chemisorbed molecules, resulting from the breaking of the O−C bonds, are present on the surface, as they should give a Si^{4+} component. This observation calls for the rupture of the Si−O bond. We recall that Si−O bond breaking is also seen in PTES dissociation on Si(001)-2 × 1.[11] Si^{3+} and Si^{2+} states are also absent from the Si 2p XPS spectrum of chemisorbed TEOS. As Si^+ is the only oxidation state observed (SCLS of +0.90 eV), three to four Si−O bonds are necessarily cleaved within the TEOS molecule, leading either to the formation of the $(Si^S)_3Si^T{-}OC_2H_5$ adduct (plus three $\equiv Si^S{-}OC_2H_5$ moieties) or to the release of an atomic silicon (plus four $\equiv Si^S{-}OC_2H_5$). However, the Si^{1+} component, due to $\equiv Si^S{-}OC_2H_5$ moieties, cannot be distinguished from $(Si^S)_3Si^T{-}OC_2H_5$ ones, the Si 2p XPS spectra themselves cannot give a definite answer on the extent of the dissociation.

The C 1s XPS spectrum ($h\nu$ = 350 eV) of TEOS chemisorbed at room temperature, see Figure 1c, is fitted with five components (fitting parameters are collected in section A, Table S2, of the Supporting Information). The very weak peak at lower BE (∼283.2 eV) can be ascribed to carbonaceous CH_x species likely due to beam damage.[25] The BE of the four main components are interpreted based on straightforward initial-state considerations as we did for PTES.[11] The α peak at 286.54 eV is attributed to carbons bonded to oxygen in ethoxy groups (Si−O−$\underline{C}H_2$−CH_3) and the β peak at 285.23 eV to terminal carbon atoms in those

dx.doi.org/10.1021/jp407411k | J. Phys. Chem. C 2014, 118, 1887−1893

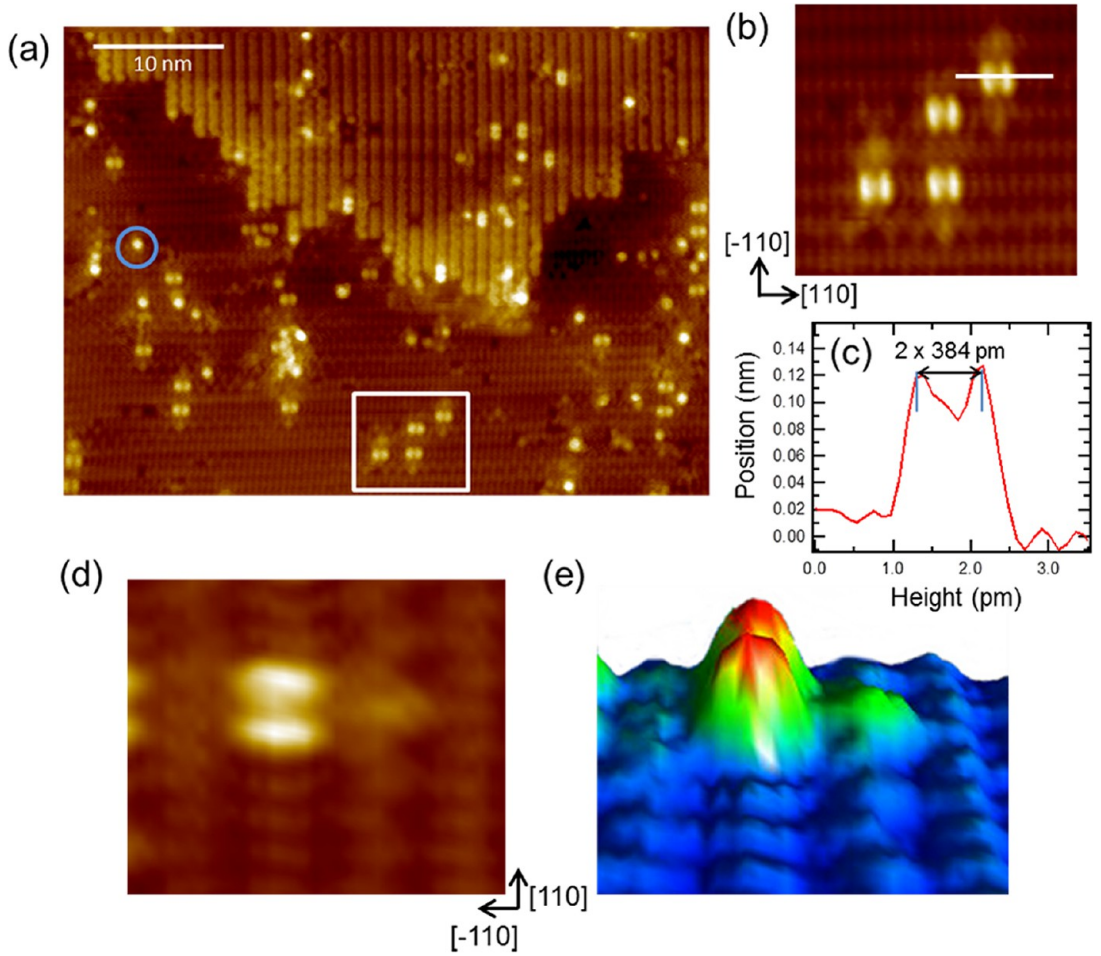

Figure 2. (a) Occupied-states STM image (V_{bias} = −2.0 V, I = 100 pA; 50 nm × 33 nm) of TEOS adsorbed on Si(001)-2 × 1 (n^+-doped, 0.003 Ω·cm) (clean surface exposed to 0.4 L of TEOS, 10 min, 9 × 10^{-10} mbar, at 300 K). The blue circle marks the position of the isolated features we attribute to nonfully dissociated TEOS. The white rectangle marks the position of four fully dissociated molecules. (b) Magnified image of the rectangular area in image (a) (8 nm × 8 nm). (c) Topographical profile along the line drawn in (b). (d) Occupied-states STM image of one adsorbed TEOS molecule, (e) with its 3D representation.

ethoxy groups (Si−O−CH_2−$\underline{C}H_3$). The ethoxy termination corresponds to ∼80% of the carbon species on the surface. The detection of surface ethoxy groups, as majority products, is consistent with the observation of a single oxidation component (Si^{1+}) in the Si 2p spectrum, confirming that Si^T−O bond breaking is the main dissociation channel. The minority product is the ethyl termination: the γ peak at 284.70 eV is attributed to the terminal carbon (Si−CH_2−$\underline{C}H_3$) and the δ peak at 284.07 eV to the carbon atom directly bonded to silicon (Si−$\underline{C}H_2$−CH_3). A similar BE shift of 0.6 eV is observed in the C 1s XPS spectrum of cyclopentene di-σ bonded on Si(001) that exhibits two components, at 284.2 eV (C bonded to Si) and at 284.8 eV (C nonbonded to Si).[28] The presence of ethyl groups needs the breaking of the O−C bond. The O 1s spectrum is not resolved enough (see Supporting Information, section B, Figure S1) to allow the detection of siloxane oxygens that could be present on the surface.

While XPS proves that the dissociative adsorption of TEOS on Si(001) surface involves (essentially) the cleavage of the Si^T−O bonds and the bonding of ethoxy groups to the surface. The nature of the adsorption sites needs to be determined by STM imagery. The silicon wafer was taken from the same batch as the one used for XPS (n^+-type, phosphorus-doped, resistivity of 0.003 Ω·cm).

We first examined the early stage of adsorption at 300 K, exposing the surface to a low TEOS dose, 0.4 L, that is, an order of magnitude less than the exposure used in XPS. This eased the identification of the adsorption sites, as large portions of the surface remain clean. In Figure 2a we show a filled state image of the surface. Two types of bright protrusions sitting on the dimer rows are observed. The minority adsorption feature (30% of the dissociation products) appears as an isolated protrusion (blue circle Figure 2a) of apparent height ∼130 pm. It seems to encompass two adjacent silicon dimers in a row. We attribute it to a nonfully dissociated molecule. This hypothesis is supported by the fact that for larger doses, these isolated protrusions are no longer seen (Figure 4). The majority of adsorption features is a pair of protrusions of height ∼109 pm (somewhat smaller than that of the preceding one). Four such pairs are enclosed in the white rectangle of Figure 2a. Each pair extends over three dimers, as the protrusion maxima are separated by 2 × 384 pm, twice the interdimer distance in a row (Figure 2b,c). The symmetry of the pairs of protrusions in the mirror planes ($\bar{1}10$) and (110) is a signature of the full TEOS dissociation where each bright protrusion is composed of two ethoxy moieties bonded to the same dimer. As much as all Si−O bonds are broken in the TEOS molecule, the fate of the released silicon atom needs to be clarified.

dx.doi.org/10.1021/jp407411k | J. Phys. Chem. C 2014, 118, 1887−1893

In Figure 2d, we zoom in on a pair of protrusions from Figure 2b. The 3D view (Figure 2e) helps show the nature of the adsorption site after molecular breaking. A weaker protrusion can be seen on the row adjacent to the ethoxy-decorated row. Its height is about 34 pm, four times smaller than the protrusions associated to the ethoxy groups. The systematic presence of this protrusion in the vicinity of the four ethoxy groups is indicative of the presence of the released silicon atom trapped on the adjacent row.

The resolution of Figure 2b is good enough to observe the influence of TEOS fragments on surface buckling. On the dimer row bearing the ethoxy groups, the dynamic buckling is not affected: the dimers appear symmetric as the STM scanning time (ms to s) is much longer than the flip-flop buckling period (ps).[29,30] In contrast, where the silicon monomer sits, a static buckling is observed. The question of static/dynamic dimer buckling upon adsorption was addressed theoretically by Wilson et al.,[31] for the adsorption of phosphine (PH_3) on Si(001). When the two fragments (H and PH_2) decorate the two silicon dangling bonds of a dimer no static buckling occurs. This is a situation similar to the (fully symmetric) bonding of two ethoxy groups on the same dimer. However, when PH_3 adsorbs datively (giving its lone pair to a down Si dimer atom), then static buckling is predicted by the calculation. Apparently, the adsorption of the silicon monomer causes a perturbation (e.g., a displacement of the pedestal silicon positions) comparable to that due to the dative bonding of phosphine.

To determine the exact position of the monomer on the surface, a theoretical approach is needed. DFT calculations were performed for two different adsorption sites of the silicon monomer. They are inspired by that previously determined by Brocks, Kelly, and Car for the clean surface.[32] The ball-and-stick result of DFT optimized configurations are shown in Figure 3 (see Supporting Information section B for more computational details). In the most stable position, the adatom is bonded to two adjacent dimers in the same row (the so-called position M in ref 32), roughly normal to a silicon of the second layer. As it can be seen in Figure 3, two dangling bonds (labeled DB) on the dimer pair are left after adsorption of the monomer. The weak protrusion in the experimental images could be due either to the monomer itself or to the two remaining tricoordinated silicon atoms in the dimer pair. Note that the four ethoxy groups are distributed over two silicon dimers separated by an empty one, which accounts for the depression between the paired protrusions in the experimental STM images (Figure 2b).

Two nonequivalent M-configurations are possible (Figure 3): the monomer can bind to the adjacent row pointing away from the ethoxy groups (M1) or toward it (M2). The corresponding adsorption energies were calculated for both configurations. After geometry optimization, the two configurations were almost degenerate (E_{ads}(M1) = 1.97 eV; E_{ads}(M2) = 2.01 eV). Apart from the position of the Si adatom, the most striking difference between the two configurations is the rotation of the ethoxy group in configuration M2 (by about 25° around the surface normal from a symmetric configuration, as in M1), due to the effective repulsion between the ethoxy group and the neighboring Si adatom.

Using as an input the M1 and M2 optimized configurations, we computed the corresponding occupied-state STM images in the framework of the Tersoff–Hamann theory.[33] The intensity of the tunnel current is proportional to the integrated density of state in the energy range $[\varepsilon_F - \Delta V, \varepsilon_F]$, where ε_F is the Fermi level and ΔV = 2 eV corresponds to the bias voltage of the experimental measurement. A density threshold ρ_0 was employed, which defines the height of the iso-density contour with respect to the atomic surface. ρ_0 was adjusted to a height of about 450 pm, which is a typical tip–surface distance in an experimental setup. The simulated STM images are presented in Figure 3b. As a preamble to any comparative discussion of the experimental and theoretical STM images, first, one must emphasize that calculations are carried out at 0 K. The simulated images correspond to an absolute minimum of energy; secondary energy minima that could be accessed at nonzero temperature via rotations of the ethoxy moieties around the Si–O and O–C axes (Figure 3) are not taken into account. In our simulation all tunneling currents are considered and represented in an intensity gray scale (the brightest corresponds to the most intense current). Therefore, we focus on the brightest spots in Figure 3b.

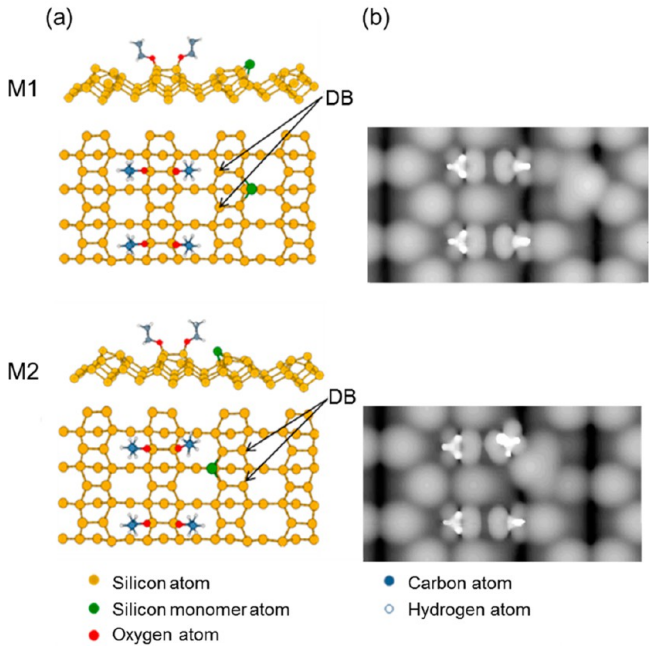

Figure 3. (a) Ball-and-stick representation of the adsorbed TEOS fragments obtained via DFT geometry optimization. M1 corresponds to the configuration in which the monomer is sitting on the dimer side opposite to the ethoxy adsorption site; M2, the monomer is pointing toward the ethoxy groups. (b) Simulated occupied-state STM images, computed within the Tersoff–Hamann approximation. Dangling bonds are denoted by DB.

The calculation gives a distinct spot for each ethoxy group, while the two ethoxy groups on a dimer are not resolved in the experimental STM images (Figure 2d). Rotations, unhindered at 300 K, may explain the difference.

The calculation gives also a crucial information: the dangling-bond bearing Si atoms (denoted DB in Figure 3a), pertaining to the two adjacent dimers on which the adatom is sitting, give a spot fainter than that of the Si adatom. In the experimental image, the faint protrusion (green in the 3D image) is seen away from the ethoxy features (Figures 2d,e). Therefore, the adatom should sit on an M1 position (and not on M2). However, in the experimental image, the faint protrusion is aligned with the depression between the two ethoxy-decorated dimers, corresponding to a bare dimer. This symmetric position of the faint protrusion is not accounted by the simulated image.

dx.doi.org/10.1021/jp407411k | J. Phys. Chem. C 2014, 118, 1887–1893

In fact, we can hypothesize that the adatom moves back and forth between two equivalent M1 positions and that the experimental image is time-averaged. The calculation of the corresponding activation dynamic barriers is ongoing.

To our knowledge, this is the first time that a silicon monomer is identified by STM on a dimer row at room temperature. Adsorption and diffusion of silicon atoms on Si(001) was widely studied, in order to gain a better knowledge of the initial stages of homoepitaxial growth.[34−38] On cold enough substrates (T = 160 K), the diffusion of the monomer is frozen out,[34] but the precise geometrical configuration of monomers likely trapped in steps, islands, or clusters cannot be obtained precisely.[39−42] At room temperature, no isolated monomer on a terrace has ever been observed, mainly because its diffusion is so fast that it cannot be imaged and thus remains unnoticed. In our case, we propose that the presence of ethoxy groups helps trapping Si adatoms on the adjacent dimer row.

We now consider what occurs for higher doses (1.2 L). The corresponding STM images are given in Figure 4. The number of paired bright protrusion corresponding to the ethoxy groups has increased significantly. The ethoxy group adsorption is clearly one-dimensional. The growth of ethoxy-decorated domains can be observed, their length extends up to ∼13 dimers. The topographical profile of Figure 4c shows that, despite the crowding, the distance between ethoxy pairs (two ⟨110⟩ lattice spacings) does not change with respect to the more diluted case (0.4 L), see Figure 2b,c.

Chemical order also appears in the direction perpendicular to the silicon dimer rows, as ethoxy-covered dimer rows alternate with ethoxy-free ones. It may be due to the presence of silicon monomers on the adjacent ethoxy-covered row. We can speculate that the TEOS molecule reacts slowly with the adatom through another channel involving C−O bond breaking. This would explain the presence of (minority) ethyl species in the C 1s XPS spectrum after a high dose of 4.5 L.

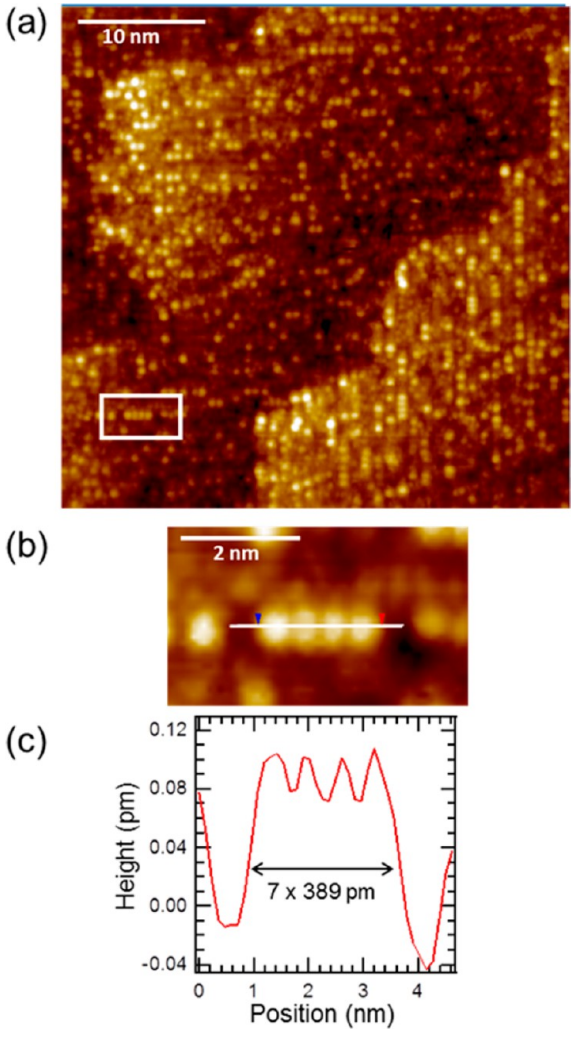

Figure 4. (a) Occupied-states STM image (V_{bias} = −2.0 V, I = 100 pA; 40 nm × 40 nm) of a TEOS adsorbed on Si(001)-2 × 1 (n^+-doped, 0.003 Ω·cm) (clean surface exposed to 1.2 L of TEOS, 30 min, 9 × 10^{-10} mbar, at 300 K). (b) Magnified image of the rectangular area of image (a). (c) Topographical profile along the line drawn in (b).

CONCLUSIONS

In this study, using XPS and STM experiments in conjunction with DFT calculations and STM image simulations, we have shown that TEOS dissociates on the Si(001)-2 × 1 surface at room temperature. For exposures in the Langmuir range, XPS shows that the majority dissociation product results from the cleavage of the Si−O bonds of the TEOS molecule. The chemical adsorption sites of the majority species are better identified by STM at low coverage (0.4 L). The four ethoxy fragments decorate two surface dimers, distant by two ⟨110⟩ lattice spacings. The remaining Si central atom moves to the adjacent dimer row, where it sits as an adatom (no ad-dimers are seen). In our DFT modeling, the adatom rests on three pedestal atoms, two silicon atoms from the top plane and one (hypercoordinated) silicon from the second plane. To account for the observed symmetries in the STM experimental image, we must assume that the monomer moves back and forth between two equivalent positions. We propose that the detection of the silicon adatom at room temperature is related to its hindered diffusion along the dimer row, due to the presence of ethoxy groups in the adjacent row. At higher coverage (1.2 L), adatom-covered rows appear nonreactive with respect to TEOS, as we observe a superstructure where ethoxy-covered dimer-rows alternate with Si adatom-occupied ones. This interesting pattern could be used to produce self-organized nanostructures on Si(001)-2 × 1.

ASSOCIATED CONTENT

Supporting Information

Experimental details (sample preparation; XPS and STM measurements), XPS curve fitting, O 1s spectrum, and computational details. This material is available free of charge via the Internet at http://pubs.acs.org.

AUTHOR INFORMATION

Corresponding Author

*(J.-J.G.) E-mail: jean-jacques.gallet@upmc.fr. Tel: +33 (0)1 44 27 66 34.

Author Contributions

The manuscript was written through contributions of all authors. All authors have given approval to the final version of the manuscript.

Notes

The authors declare no competing financial interest.

REFERENCES

(1) Yoshinobu, J.; Tsuda, H.; Onchi, M.; Nishijima, M. Rehybridization of Acetylene on the Si(111)(7 × 7) Surface: a Vibrational Study. *Chem. Phys. Lett.* **1986**, *130*, 170−174.

(2) Buriak, J. M. Organometallic Chemistry on Silicon and Germanium Surfaces. *Chem. Rev.* **2002**, *102*, 1271−1308.

(3) Filler, M. A.; Bent, S. F. The Surface as Molecular Reagent: Organic Chemistry at the Semiconductor Interface. *Prog. Surf. Sci.* **2003**, *73*, 1−56.

(4) Hersam, M.; Guisinger, N.; Lyding, N. Silicon-Based Molecular Nanotechnology. *Nanotechnology* **2000**, *11*, 70−76.

(5) Vilan, A.; Yaffe, O.; Biller, A.; Salomon, A.; Kahn, A.; Cahen, D. Molecules on Si: Electronics with Chemistry. *Adv. Mater.* **2010**, *22*, 140−159.

(6) Ulman, A. *An Introduction to Ultrathin Organic Films From Langmuir-Blodgett to Self-Assembly*; Academic Press: Boston, MA, 1991.

(7) Sagiv, J. Organized Monolayers by Adsorption. 1. Formation and Structure of Oleophobic Mixed Monolayers on Solid Surfaces. *J. Am. Chem. Soc.* **1980**, *102*, 92−98.

(8) Sugimura, H.; Hozumi, A.; Kameyama, T.; Takai, O. Organosilane Self-Assembled Monolayers Formed at the Vapor/Solid Interface. *Surf. Interface Anal.* **2002**, *34*, 550−554.

(9) Fan, C.; Lopinski, G. P. STM and HREELS Investigation of Gas Phase Silanization on Hydroxylated Si(100). *Surf. Sci.* **2010**, *604*, 996−1001.

(10) Gallet, J.-J.; Bournel, F.; Rochet, F.; Köhler, U.; Kubsky, S.; Silly, M. G.; Sirotti, F.; Pierucci, D. Isolated Silicon Dangling Bonds on a Water-Saturated n^+ Doped Si(001)-2 × 1 Surface: An XPS and STM Study. *J. Phys. Chem. C* **2011**, *115*, 7686−7693.

(11) Gallet, J.-J.; Bournel, F.; Pierucci, D.; Bonato, M.; Khaliq, A.; Rochet, F.; Silly, M.; Sirotti, F. A Synchrotron Radiation X-ray Photoemission Spectroscopy Study of n-Propyltriethoxysilane Adsorption on Si(001)-2 × 1 at Room Temperature. *J. Phys. Chem. C* **2010**, *114*, 21450−21456.

(12) Rauscher, H. The Interaction of Silanes with Silicon Single Crystal Surfaces: Microscopic Processes and Structures. *Surf. Sci. Rep.* **2001**, *42* (6), 207−328.

(13) Doering, R.; Nishi, Y. *Handbook of Semiconductor Manufacturing Technology*; CRC Press: Boca Raton, FL, 2007.

(14) Ray, S. K.; Maiti, C. K.; Lahiri, S. K.; Chakrabarti, N. B. TEOS-based PECVD of Silicon Dioxide for VLSI Applications. *Adv. Mater. Opt. Electron.* **1996**, *6*, 73.

(15) Maeda, K.; Fisher, S. M. CVD TEOS/O3 Development History and Applications. *Solid State Technol.* **1993**, *6*, 83.

(16) Bonzel, H. P.; Pirug, G.; Verhasselt, J. Low Temperature Growth of SiO_2 Films on Si(100) Using a Hot Molecular Beam of Tetraethoxysilane. *Chem. Phys. Lett.* **1997**, *271*, 113.

(17) Danner, J. B.; Rueter, M. A.; Vohs, J. M. Pathways and Intermediates in the Reaction of Tetraethoxysilane on Silicon(100)-2 × 1. *Langmuir* **1993**, *9*, 455−459.

(18) Perdew, J. P.; Wang, Y. Accurate and Simple Analytic Representation of the Electron-Gas Correlation Energy. *Phys. Rev. B* **1992**, *45*, 13244.

(19) Kresse, G.; Furthmuller, J. Efficient Iterative Schemes for ab-Initio Total-Energy Calculations Using a Plane-Wave Basis Set. *Phys. Rev. B* **1996**, *54*, 11169.

(20) Kresse, G.; Hafner, J. Ab initio Molecular Dynamics for Liquid Metals. *Phys. Rev. B* **1993**, *47*, 558.

(21) Landemark, E.; Karlsson, C.; Chao, Y.-C.; Uhrberg, R. Core-Level Spectroscopy of the Clean Si(001) Surface-Charge-Transfer within Asymmetric Dimers of the 2 × 1 and c(4 × 2) Reconstructions. *Phys. Rev. Lett.* **1992**, *69*, 1588−1591.

(22) Himpsel, F. J.; Meyerson, B. S.; McFeely, F. R.; Morar, J. F.; Taleb-Ibrahimi, A.; Yarmoff, J. A. In *Proceedings of Enrico Fermi School on Photoemission and Adsorption Spectroscopy of Solids and Interfaces with Synchrotron Radiation*; Campana, M., Rosei, R., Eds.; IOS Press, Amsterdam, Netherlands, 1992.

(23) Himpsel, F.; McFeely, F. R.; Taleb-Ibrahimi, A.; Yarmoff, J. A.; Hollinger, G. Microscopic Structure of the SiO_2/Si Interface. *Phys. Rev. B* **1988**, *38*, 6084.

(24) Jolly, F.; Rochet, F.; Dufour, G.; Grupp, C.; Taleb-Ibrahimi, A. Oxidized Silicon Surfaces Studied by High Resolution Si 2p Core-Level Photoelectron Spectroscopy using Synchrotron Radiation. *J. Non-Cryst. Solids* **2001**, *280*, 150−155.

(25) Pasquarello, A.; Hybertsen, M. S.; Car, R. Si 2p Core-Level Shifts at the Si(001)-SiO_2 Interface: A First Principles Study. *Phys. Rev. B* **1996**, *53*, 10942−10950.

(26) Yazyev, O. V; Pasquarello, A. Origin of Fine Structure in Si 2p Photoelectron Spectra at Silicon Surfaces and Interfaces. *Phys. Rev. Lett.* **2006**, *96*, 157601.

(27) Jolly, W. L.; Bomben, K. D.; Eyermann, C. J. Core-Electron Binding Energies for Gaseous Atoms and Molecules. *Atom. Data Nucl. Data* **1984**, *31*, 433−493.

(28) Khaliq, A.; Pierucci, D.; Tissot, H.; Gallet, J.-J.; Bournel, F.; Rochet, F.; Silly, M.; Sirotti, F. Ene-Like Reaction of Cyclopentene on Si(001)-2 × 1: an XPS and NEXAFS Study. *J. Phys. Chem. C* **2012**, *116*, 12680−12686.

(29) Weakliem, P. C.; Carter, E. A. Constant Temperature Molecular Dynamics Simulations of Si(100) and Ge(100): Equilibrium Structures and Short-Time Behaviour. *J. Chem. Phys.* **1992**, *96*, 3240−3250.

(30) Hamers, R. J.; Wang, Y. Atomically-Resolved Chemistry and Bonding of Silicon Surfaces. *Chem. Rev.* **1996**, *96*, 1261−1290.

(31) Wilson, H. F.; Marks, N. A.; McKenzie, D. R. Defect-Induced Dimer Pinning on the Si(001) Surface. *Surf. Sci.* **2005**, *587*, 185−192.

(32) Brocks, G.; Kelly, P. J.; Car, R. Binding and Diffusion of a Si Adatom on the Si(100) Surface. *Phys. Rev. Lett.* **1991**, *66*, 1729.

(33) Tersoff, J.; Hamann, D. R. Theory of the Scanning Tunneling Microscope. *Phys. Rev. B* **1985**, *31*, 805.

(34) Wolkow, R. A. Evidence of Adsorbed Atom Pairing during Homoepitaxial Growth of Silicon. *Phys. Rev. Lett.* **1995**, *74*, 4448.

(35) Zhang, Z.; Wu, F.; Lagally, M. G. An Atomistic View of Si(001) Homoepitaxy. *Annu. Rev. Mater. Sci.* **1997**, *27*, 525.

(36) Wang, Y.; Bronikowski, M. J.; Hamers, R. J. An Atomically Resolved Scanning Tunneling Microscopy Study of the Thermal Decomposition of Disilane on Si(001). *Surf. Sci.* **1994**, *311*, 64.

(37) Vasek, J. E.; Zhang, Z. Y.; Salling, C. T.; Lagally, M. G. Effects of Hydrogen Impurities on the Diffusion, Nucleation, and Growth of Si on Si(001). *Phys. Rev. B* **1995**, *51*, 17207.

(38) Fehrenbacher, M.; Spitzmüller, J.; Memmert, U.; Rauscher, H.; Behm, R. J. Interaction of SiH_4 with Si(100)2 × 1 and with Si(111)7 × 7 at 690 K: A Comparative Scanning Tunneling Microscopy Study. *J. Vac. Sci. Technol. A* **1996**, *14*, 1499.

(39) Mo, Y. W.; Kleiner, J.; Webb, M. B; Lagally, M. G. Surface Self-Diffusion of Si on Si(001). *Surf. Sci.* **1992**, *268*, 275.

(40) Swartzentruber, B. S. Kinetics of Si Monomer Trapping at Steps and Islands on Si(001). *Phys. Rev. B* **1997**, *55*, 1322.

(41) Swartzentruber, B. S. Direct Measurement of Surface Diffusion Using Atom-Tracking Scanning Tunneling Microscopy. *Phys. Rev. Lett.* **1996**, *76*, 459.

(42) Bedrossian, P. J. Si Binding and Nucleation on Si(100). *Phys. Rev. Lett.* **1995**, *74*, 3648.